REPORT DOCUMENTATION PAGE

Form Approved
OMB No. 0704-0188

1. AGENCY USE ONLY (Leave blank)	2. REPORT DATE	3. REPORT TYPE AND DATES COVERED
	10-16-97	Final Technical Report, 8/15/94-8/14/97

4. TITLE AND SUBTITLE
Designing Optimal Actuation and Sensing Systems
(FY 94 AASERT)

5. FUNDING NUMBERS
(G)F49620-94-1-0346
AFOSR-TR-97
0651

6. AUTHOR(S)
Dr. Harley H. Cudney

7. PERFORMING ORGANIZATION NAME(S) AND ADDRESS(ES)
Interdisciplinary Center for Applied Mathematics
Wright House, West Campus Drive
Virginia Polytechnic Institute and State University
Blacksburg, VA 24061-0531

8. PERFORMING ORGANIZATION REPORT NUMBER

9. SPONSORING/MONITORING AGENCY NAME(S) AND ADDRESS(ES)
Air Force Office of Scientific Research
Code NM
110 Duncan Avenue, Suite B115
Bolling Air Force Base, DC 20332

10. SPONSORING/MONITORING AGENCY REPORT NUMBER

11. SUPPLEMENTARY NOTES

12a. DISTRIBUTION/AVAILABILITY STATEMENT
UNLIMITED

12b. DISTRIBUTION CODE

13. ABSTRACT (Maximum 200 words)

This final technical report contains a summary and highlights on research funded by the AFOSR under grant F49620-94-1-0346, titled "Designing Optimal Actuation and Sensing Systems (FY94 AASERT). This AASERT grant supported three graduate students to work on the following topic: 1) developing design procedures for model reference adaptive control, 2) designing and building an adaptive vibration absorber, and 3) supporting the Air Force Philips Laboratory by designing optimal active structural acoustic control for new composite rocket fairings. The following results were obtained. We developed a general method for designing an MRAC controller applied to a second order SISO plant. An adaptive self-tuning vibration absorber was designed, built, modeled, and tested. We created a modeling technique for the interior acoustic noise levels of rockets during launch, and tested a simply supported cylinder.

14. SUBJECT TERMS	15. NUMBER OF PAGES
OPTIMAL DESIGN, ADAPTIVE STRUCTURES, ACTIVE ACOUSTIC CONTROL	20
	16. PRICE CODE

17. SECURITY CLASSIFICATION OF REPORT	18. SECURITY CLASSIFICATION OF THIS PAGE	19. SECURITY CLASSIFICATION OF ABSTRACT	20. LIMITATION OF ABSTRACT
Unclassified	Unclassified	Unclassified	UL

FINAL TECHNICAL REPORT

AFOSR GRANT: F49620-94-1-0346

ADAPTIVE METHODS FOR OPTIMAL DESIGN
(FY94 AASERT)

AIR FORCE CENTER FOR OPTIMAL DESIGN AND CONTROL

for the period

15 August 1994 - 14 August 1997

Submitted to:

Air Force Office of Scientific Research
Mathematical and Computer Sciences
110 Duncan Avenue, Suite B115
Bolling Air Force Base, DC 20332-0001

Submitted by:

Dr. Harley H. Cudney

Air Force Center for Optimal Design and Control
Virginia Polytechnic Institute and State University
Wright House, West Campus Drive
Blacksburg, VA 24061-0531

October 17, 1997

Final Technical Report

Objectives

This project was funded through an AFOSR AASERT grant and supported four graduate students to work with Prof. Harley H. Cudney. The overall objective of the grant was to develop new technologies in optimal actuation and sensing methods. The specific objective of the grant was to develop a working relationship with an Air Force Laboratory and actively perform research that specifically supported their mission.

The project that was originally identified which most closely supported the mission of the Structures and Dynamics Branch of the Air Force Phillips Laboratory at Kirkland Air Force Base was to develop control algorithms to test on the space-flight experiment ASTREX. However, another requirement that the project must satisfy is to have a research topic suitable for the student to write a dissertation. After discussions with Dr. Alok Das, and Capt. Jeanine Sullivan, Ph.D., we determined the ASTREX project did not have this content. In subsequent discussions, we identified the acoustic control of fairings as being a definite technology need for both the Air Force and industry.

To fulfill the overall objective of developing new technologies for optimal actuation and sensing, we investigated developing design procedures for model reference adaptive control, which has been widely adopted in the structures community as a robust control method. However, no specific design procedures exist. Our objective was to develop a design procedure and assess the robustness of four approaches to control: a classical pole placement method, and three adaptive control approaches.

Also to support of our overall objective, an adaptive vibration absorber capable of detecting the frequency of the force and tuning itself automatically to that particular frequency, is designed, built, and tested.

Status

Design methods for Model Reference Adaptive Control: Concluded

The Model Reference Adaptive Control Project is complete and summarized below. Mr. Jon Hill graduated with a Master's Degree in Mechanical Engineering in 1995.

Adaptive Vibration Absorbers: Concluded

An adaptive vibration absorber was designed, built, and tested. A model was developed and this model was used to develop the tuning algorithm. The actively controlled absorber was tested and shown significant performance advantages over passive absorbers.

Active Acoustic Control of Rocket Payload Fairings: Continuing

A formulation was created for the active acoustic control problem. We consider cylinders to be an effective model of a rocket fairing. We have developed an analytical method to predict the noise level inside the cylinder due to acoustic excitation. We have also created a cylinder which has simply supported boundary conditions. Both of these steps are necessary to determine the control authority of piezoelectric actuators for providing effective attenuation of the acoustic loads due to the rocket being launched.

Accomplishments, New Findings, and Research Highlights

Design methods for Model Reference Adaptive Control

In this study, we assessed the robustness of four distinct control approaches: pole placement; the command generator tracker (CGT) approach to model reference control; model reference adaptive control (MRAC); and MRAC using a fixed feedback gain. We use a second order, single-input single-output (SISO) plant to examine the performance and stability of each method. This evaluation spans a broad range of design goals and uncertainty in models of the plant.

Pole placement and CGT designs are linear and relatively easy to implement, but require explicit knowledge of the plant. Although MRAC schemes require little knowledge of the plant's dynamic characteristics, such algorithms are non-linear and involve design variables whose effects are not readily apparent. Currently, there are no general design procedures for MRAC. In this study, we propose a method for designing an MRAC controller applied to a second order SISO plant. This method does not require the controller to be tuned for different closed-loop performance goals. This procedure also creates a consistent basis for comparing the robustness of all four algorithms.

Pole placement and the CGT control perform as designed if the plant is modeled correctly. Under this circumstance, the adaptive controllers also perform at levels equivalent to the linear algorithms. However, conditions with plant modeling error highlight enormous differences among the four algorithms. Pole placement suffers the largest response error and for extreme testing conditions, instability. The CGT controller exhibits better performance than pole placement and remains stable over all testing variables. MRAC maintains a high performance level under severe testing conditions. MRAC requires minimal plant knowledge to guarantee stability and good performance.

Our model reference adaptive control design procedure yielded excellent results in simulation. Considerations of representative model trajectories, representative output error, sampling time, and transient response time factored into our weighting matrix selection. We used Lyapunov stability to results to determine a feedthrough term, minimizing the effects of plant modeling error. In the presence of plant modeling error, these design considerations were sufficient to produce responses well correlated with the reference model's. The model reference adaptive controller performed particularly well over long transient periods, where the adaptive gains could accurately converge to values minimizing output error.

A major benefit of our design procedure is the absence of user-controller interaction. This procedure only requires an approximate model of the plant and a specified reference model. Although our study assumes a very simple system, where the reference model and plant are both second order, this design method is innovative and may be applied to a larger class of systems.

In the comparative analysis of robustness, we found that generally, adaptive control exceeds the ability of linear controllers to track the response of the reference model. Although the linear model reference control method yielded lower performance indexes periodically, the adaptive methods begin to track the model output in fewer time steps than the linear methods. This attribute of adaptive control is advantageous, but not sufficiently recognized by our quantitative evaluation.

We raised two issues worthy of further investigation. First, we should examine the effects of signal noise for a particular choice of representative error. Our selection was very low, resulting in a relatively high feedback weighting value. This high computational value did not pose a problem in our "sterile" testing environment. However, it is possible to achieve equitable performance for lower feedback weighting values.

The two types of MRAC schemes produced similar results. We hypothesized that MRAC, using a fixed feedback gain, would have a lower sensitivity to noise than the fully adaptive version. The fully adaptive MRAC performed marginally better than its counterpart in our study. We should reexamine these methods under more realistic testing conditions.

We did not attempt control for an input to the reference model. Our design procedure can be easily modified to account for this. Using a reference model command, the plant has a non-zero steady state. This gives the designer a perspective to better evaluate and design the ratio between proportional and integral weighting matrices. A non-zero steady state also accentuates the benefits of adaptive control over linear control.

Adaptive Vibration Absorbers

An adaptive vibration absorber capable of detecting the frequency of the force and tuning itself automatically to that particular frequency, is designed, modeled, and tested. The design stage begins with a criteria list that evaluates various design concepts. After a concept is chosen, the concept is developed using vibration theory and beam equations. The principal system is designed first to obtain a certain natural frequency. The absorber is designed next so that its range of frequencies includes the natural frequency of the principal system. The design consists of a cantilever beam as the principal system, and an assembly of three rods and a motor as the vibration absorber.

Preliminary component testing was performed to develop a model of the principal system, absorber system, and the combined (principal and absorber) system. The models predict the natural frequencies of the systems, and in the case for the combined system, the model predicts the anti-resonant and resonant frequencies. Experiments of the

combined system were performed to evaluate the effectiveness of the absorber. Furthermore, experimental results for all three systems were compare to the results from the theoretical model.

The combined system evaluation shows that the absorber works effectively. It is able to include the natural frequency of the principal system in its range of frequencies. The model predicts the anti-resonant frequency within a mean of 0.3 % error. Furthermore, the model predicts the two resonant frequencies (ω_1 and ω_2) within a mean of 0.6 % error and 0.6 % error, respectively.

A control algorithm is developed and applied to this tunable vibration absorber. The adaptive vibration absorber is capable of detecting the frequency of the driving force and tuning itself automatically to that frequency. The primary structure was previously designed to obtain a certain natural frequency, and the absorber was designed such that its range of frequencies included the natural frequency of the primary structure. The primary structure consists of a cantilevered beam with the absorber attachment hardware, and the vibration absorber assembly consists of three rods and a stepper motor.

The control algorithm uses a look-up table and a gradient search to optimize the effectiveness of the absorber to reduce the vibrations on the primary structure. The look-up table uses an equation which is based on experimental data to transform a given voltage input (directly proportional to the forcing frequency) into an output command necessary to adjust the natural frequency of the absorber. One the input voltage reaches steady state, the gradient search routine adjusts the natural frequency of the absorber to ensure the absorber is tuned to the optimal frequency that minimizes the vibration amplitude of the primary structure.

The primary structure with the adaptive absorber offers significant reductions in the vibration amplitudes of the primary structure, as compared to the primary structure with no absorber, and **to the primary structure with a passive absorber.**

Active Acoustic Control of Rocket Payload Fairings

Future launch vehicle payload fairings will be manufactured from advanced lightweight composite materials. The loss of distributed mass causes a significant increase in the internal acoustic environment, causing a severe threat to the payload. During launch the payload fairing is excited by a severe acoustic loading provided from the burn of the rocket engines. The acoustic noise is transmitted through the fairing and creates an internal SPL ranging from 120 to 140 dB that can damage the payload. There remains a great deal of work in understanding the Physics behind the acoustical problem and the interaction between the external and internal SPL's and the payload fairing skin. Current state of the art active control technology has been considered to tackle the fairing acoustical problem. The actuator types evaluated include acoustical noise sources, point forces, magnetostrictive actuators, smart materials, electrostrictive and piezoelectric actuators. Currently the best candidate to solve the problem is the piezoelectric actuator. However, due to the broadband and intense nature of the acoustic environment, it remains uncertain if piezoelectric actuators will have the authority to solve the problem.

To help determine the acoustic control authority of piezoelectric actuators mounted on a rocket fairing, the internal acoustic response created by the actuators needs to be determined. The internal acoustic response of a closed simply-supported cylinder actuated by piezoelectric actuators can be conveniently determined by using the Kirchoff-Helmholtz integral and the cylinder's spatial surface velocity. The surface velocity is determined using an impedance model of an actuator bonded to the surface of a cylinder. The structural analysis is compared to an experiment and the results are in agreement. The acoustic formulation is described along with a description of future work. The work presented provides the initial steps required in determining the acoustic authority and feasibility of using piezoelectric actuators on rocket fairings.

The structural model we developed needs to be further verified for a broader frequency range with more experimental information about the absolute spatial displacement of the cylinder. This can be accomplished by using scanning laser vibrometry. The model also needs to be verified for out of phase actuation and more attention needs to be given to the actual damping values on a mode for mode basis. The results from the impedance model will ultimately be used to calculate the acoustic response within the cylinder. Once the acoustic model is verified, the combined structural/analytical model will be used to determine the authority of PZT actuators on a cylinder with properties similar to a rocket payload fairing.

An experiment of a cylinder with simply-supported boundary conditions has been conducted and was shown to exhibit dynamic behavior very similar to what the theory predicts. An analytical impedance based model of a PZT actuating on a SS cylinder was also described and compared with the experimental results. The results indicate that the impedance based model can predict the overall resonant and modal behavior but, more importantly for acoustical applications, is able to determine the magnitude of the vibration. An acoustical formulation of the pressure field within the cylinder has also been described based on the Kirchoff-Helmholtz integral. The work presented provides the initial steps required in determining the acoustic authority and feasibility of using piezoelectric actuators on rocket fairings.

In many aerospace and structural applications, idealized cylinders are used to approximate more complex structures such as airplane fuselages and rocket payload fairings. Many authors have created sophisticated models of the structural response of cylinders excited by a variety of actuators. However seldom are these models verified experimentally. None of the models created to describe the response of a simply-supported (SS) cylinder have ever been verified. In this work several different boundary conditions are created to approximate an ideal SS cylinder. The different boundary conditions tested are described and compared with finite element analysis (FEA) and with an impedance based analytical model for a piezoelectric actuator (PZT) exciting a SS cylinder. The work presented describes the steps taken in creating a physical boundary condition which approximates the ideal boundary condition for a SS cylinder. The results indicate that the created physical boundary condition resembles the ideal SS boundary condition. The structural response computed by the impedance model is also shown to agree with the experiment and with the FEA. The results can be used to create other experimental SS cylinders and will be used at Virginia Tech to determine the feasibility of applying piezoelectric actuators to control rocket payload fairings vibrations.

The work presented describes the steps taken in creating a physical boundary condition which approximates the ideal boundary condition for a SS cylinder. The results indicate that the created physical boundary condition resembles the ideal SS boundary condition but is not perfect. It does however have very similar vibrating properties and modal distribution. The analytical model predicts the expected physical changes to the response as the actuator location is shifted. The structural response computed by the impedance model is also shown to be similar to the experimental response and matches the natural frequencies determined using FEA. The results can be used to create other experimental SS cylinders and will be used at Virginia Tech to determine the feasibility of applying piezoelectric actuators to control rocket payload fairings vibrations.

Personnel Supported

Mr. Jon Hill, M.S. student in Mechanical Engineering, graduated 8/95.

Ms. Ana Moyka, M.S. student in Mechanical Engineering, graduated 2/96.

Mr. Rodney Red-Wing, M.S. student in Mechanical Engineering, partly supported on minority scholarship and partly via this AASERT, graduated 5/97

Mr. Chris Niezrecki, Ph.D. student in Mechanical Engineering

Publications (peer-reviewed)

Thesis: A Design Procedure for Model Reference Adaptive Control by Jonathan Hill, August 1995

Thesis: Adaptive Self-Tuning Vibration Absorber by Rodney Red Wing, May 1997.

Thesis: Adaptive Vibration Absorber by Ana S. Moyka, June 1994

Niezrecki, C.,* and H. H. Cudney, 1997. "Structural Control Using Analog Phase-Locked Loops," ASME Journal of Vibration and Acoustics, 119(1), pp. 104-109.

Niezrecki, C., and H. H. Cudney, 1994, "Improving the Power Consumption Characteristics of Piezoelectric Actuators," Journal of Intelligent Material Systems and Structures, 5(4), pp. 522-529.

Messer, R. A., R. T. Haftka, and H. H. Cudney, 1994, "The Cost of Model Reference Adaptive Control: Analysis, Experiments, and Optimization," AIAA Journal of Guidance, Control and Dynamics, 1994, 17(5)

Niezrecki, C., and H. H. Cudney, 1997. "Active Control Technology Applied to Rocket Fairing Structural Vibrations and Acoustics," Proc. of the AIAA/ASME/AHS Adaptive Structures Forum, Kissimmee, FL, April 7-10. Published by the American Institute of Aeronautics and Astronautics (AIAA), Reston, VA, pp. 1525-1535.

Niezrecki, C., and H. H. Cudney, 1998, "Creating and Verifying a Research-Grade Simply-Supported Cylinder with Applications to Aerospace Structures", to be presented at the 1998 International Modal Analysis Conference, Santa Barbara, Feb.

Niezrecki, C., and H. H. Cudney, 1997. "Active Control Technology Applied to Rocket Fairing Structural Vibrations and Acoustics," Proc. of the AIAA/ASME/AHS Adaptive Structures Forum, Kissimmee, FL, April 7-10. Published by the American Institute of Aeronautics and Astronautics (AIAA), Reston, VA, pp. 1525-1535.

(Please note: This paper is attached to this report).

Niezrecki, C., and H. H. Cudney, 1994, "Application of an Analog Phase Lock Loop to the Modal Control of Mechanical Structures," Adaptive Structures and Material Systems: Analysis and Applications, edited by E. Garcia, H. H. Cudney and A. Dasgupta, AD-Vol. 45 and MD-Vol. 54, American Society of Mechanical Engineers, New York, NY, pp. 235-246, and presented at the Adaptive Structures and Composite Materials Symposium, ASME International Congress and Exposition, November 6-11, Chicago, IL.

Diehl, G., and H. H. Cudney, 1994, "The Effects of Shaped Piezoceramic Actuators on the Excitations of Beams," Proc. of the AIAA/ASME Adaptive Structures Forum, Hilton Head, SC, April 21-22. Published by the American Institute of Aeronautics and Astronautics (AIAA), Reston, VA, pp. 270-278.

Interactions and Transitions

Continuing to work closely with Dr. Alok Das and Capt. Jeanine Sullivan at the Air Force Philips Laboratory in Albuquerque, NM. Our most recent interaction was a teleconference between Virginia Tech and the Philips Laboratory, where Mr. Chris Niezrecki presented his dissertation proposal.

New Discoveries, Inventions, and Patent Disclosures

None.

Honors and Awards

None.

ACTIVE CONTROL TECHNOLOGY APPLIED TO ROCKET FAIRING STRUCTURAL VIBRATIONS AND ACOUSTICS

Christopher Niezrecki* **& Harley H. Cudney****
Department of Mechanical Engineering
Virginia Polytechnic Institute and State University
Blacksburg, Virginia 24061

Abstract

Future launch vehicle payload fairings will be manufactured from advanced lightweight composite materials. The loss of distributed mass causes a significant increase in the internal acoustic environment, causing a severe threat to the payload. Using piezoelectric actuators to control the fairing vibration and the internal acoustic environment has recently been proposed. The control authority of these actuators for this problem has not yet been determined. To help determine the acoustic control authority of piezoelectric actuators mounted on a rocket fairing, the internal acoustic response created by the actuators needs to be determined. The internal acoustic response of a closed simply-supported cylinder actuated by piezoelectric actuators can be conveniently determined by using the Kirchoff-Helmholtz integral and the cylinder's spatial surface velocity. The surface velocity is determined using an impedance model of an actuator bonded to the surface of a cylinder. The structural analysis is compared to an experiment and the results are in agreement. The acoustic formulation is described along with a description of future work. The work presented provides the initial steps required in determining the acoustic authority and feasibility of using piezoelectric actuators on rocket fairings.

Introduction

Traditionally, payload fairings have been constructed from lightweight aluminum alloys. However, designers are currently developing composite fairings which are much easier to manufacture while also being lighter and stiffer than existing aluminum fairings.

Reducing the acoustic noise that the payload (i.e. satellite) receives during launch has always been an important design constraint. An excess of acoustic noise transmitted through the fairing poses a potential threat to the life of the payload. Since future fairings will be constructed of lighter materials having a lower transmission loss (TL), the acoustic threat is even more severe. The most recent research for the problem has implemented passive techniques in the form of improved blankets and dynamic vibration absorbers mounted on the payload[1-5].

Active control technology is currently being investigated as a potential solution for the fairing acoustic problem in the low frequency range (50-400 Hz) where blankets are less effective. A review of current active control actuators has been recently performed along with a description of the acoustic fields needing control[6]. The use of piezoelectric (PZT) actuators to actively control fairing structural vibrations and the internal acoustic environment has recently been proposed. However, the authority of these actuators for this problem has not yet been determined. To help determine the acoustic control authority of PZT actuators mounted on fairing like structures, the internal acoustic response created by the actuators needs to be determined. For a closed cylinder, this can be accomplished by using the Kirchoff-Helmholtz (K-H) integral once the spatial structural response is determined. A similar analysis has been performed, but only implemented harmonic point load excitation[7].

Presented within this paper is a description of the theoretical analysis used to determine the structural response of a simply-supported (SS) cylinder via an impedance based model for the PZT actuator. The theoretical solution of the internal acoustic field using the structural response is also discussed along with some advantages of using this technique. An experiment is performed to validate the structural model and the empirical and analytical results are compared. To the author's knowledge an analytical/experimental comparison of a SS cylinder has not been performed. Finally the major findings and future work are presented.

Theoretical Development

PZT Actuator Model and Structural Response

* Graduate Research Assistant

** Associate Professor of Mechanical Engineering, Member AIAA

Theoretical Development

PZT Actuator Model and Structural Response

Several models for PZT actuator patches attached to cylinders have been presented. Initially plate models were adapted to cylinders via the Donnel-Mushtari and Love shell equations[8,9]. Later models were based on shell governing equations[10-12]. All of these models are based on force inputs calculated at zero frequency excitation. None of them take into consideration the changing impedance of the structure as a function of frequency. This will lead to an incorrect response if the structural impedance changes with frequency. Impedance models of PZT actuators have been previously developed for beams, plates, rings and shells[13-19]. It has been shown that neglecting the frequency varying structural impedance can lead to an incorrect response. The structural response of a SS cylinder is determined using the impedance model developed by Lalande[19]. A general overview of this model will now be presented.

The coordinate system used for the cylinder and actuator is shown in Fig. 1. The model assumes two rectangular PZT actuators are attached to the cylinder, one on the outer surface and another collocated on the inner surface. The resultant forces (in phase actuation) and moments (out of phase actuation) are assumed to act at the cylinder's midplane as shown in Fig. 2.

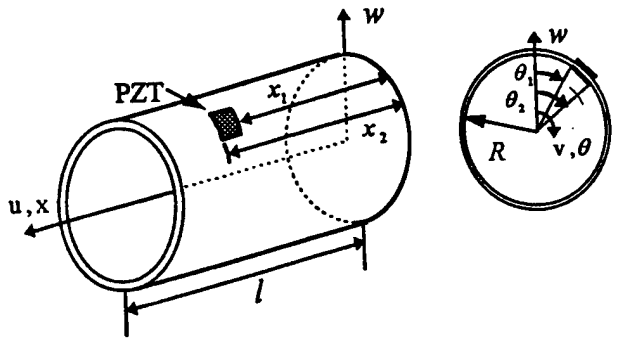

Figure 1. Cylinder with Mounted Actuators

The relationship between the actuator output force and the equivalent midplane force or moment in the axial or tangential direction is given by:

inphase:

$$N_x = 2F_x \tag{1a}$$

$$N_\theta = 2F_\theta \tag{1b}$$

out of phase:

$$M_x = (t_a + t_s)F_x \tag{1c}$$

$$M_\theta = (t_a + t_s)F_\theta \tag{1d}$$

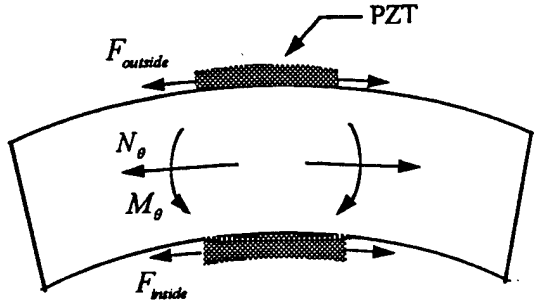

Figure 2. Transfer of Actuator Forces to Equivalent Mid-Plane Loading

where t_a and t_s are the actuator and shell thickness, respectively. The actuator forces F_x and F_θ need to be solved by using the PZT actuator constitutive equations, actuator impedance and the structural impedance or admittance (see Fig. 3). The structural impedance along the actuator edge is related to the structural admittance by:

$$\begin{bmatrix} Z_{xx} & Z_{x\theta} \\ Z_{\theta x} & Z_{\theta\theta} \end{bmatrix} = \begin{bmatrix} H_{xx} & H_{x\theta} \\ H_{\theta x} & H_{\theta\theta} \end{bmatrix}^{-1} \tag{2}$$

where Z and H represent the structural impedance and admittance, respectively. The structural admittance will be discussed later. The input impedance (shorted) of the PZT actuators are given by:

direct terms:

$$Z_{axx} = \frac{Y_a^E t_a \kappa R_a}{i\omega \tan(\kappa l_a)} \tag{3a}$$

$$Z_{a\theta\theta} = \frac{Y_a^E t_a \kappa l_a}{i\omega \tan(\kappa R_a)} \tag{3b}$$

cross terms:

$$Z_{ax\theta} = \frac{Y_a^E t_a \kappa l_a}{i\omega \tan(\kappa l_a)} \tag{3c}$$

$$Z_{a\theta x} = \frac{Y_a^E t_a \kappa R_a}{i\omega \tan(\kappa R_a)} \tag{3d}$$

where, Y_a^E is the actuator complex modulus of elasticity with no applied electric field, R_a is the actuator angular length, l_a is the actuator axial length,

ω represents the angular frequency, i is an imaginary number, and κ is given by:

$$\kappa = \omega\sqrt{\rho_a / Y_a^E} \tag{4}$$

where, ρ_a is the density of the actuator.

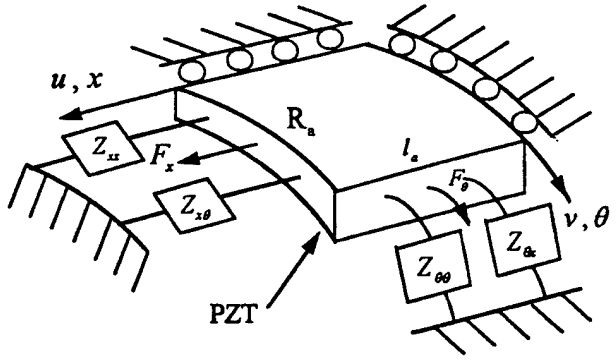

Figure 3. Interaction Between the PZT and the Cylinder via the Structural Impedance

Combining the actuator impedances, Eq. 3, with the PZT constitutive equations and applying boundary conditions, a relationship between the dynamic actuator force and the structural impedance (Eq. 2) results[17,19]:

$$F_x = \frac{-i\omega}{R_a}\left(A\sin(\kappa l_a)Z_{xx} + C\sin(\kappa R_a)Z_{x\theta}\right)e^{i\omega t} \tag{5a}$$

$$F_\theta = \frac{-i\omega}{l_a}\left(A\sin(\kappa l_a)Z_{\theta x} + C\sin(\kappa R_a)Z_{\theta\theta}\right)e^{i\omega t} \tag{5b}$$

where, A and C are calculated from,

$$\begin{Bmatrix} A \\ C \end{Bmatrix} = \begin{bmatrix} \kappa\cos(\kappa l_a)\left(1 - \nu_a \frac{Z_{x\theta}}{Z_{ax\theta}} + \frac{Z_{xx}}{Z_{axx}}\right) \\ \kappa\cos(\kappa l_a)\left(\frac{Z_{x\theta}}{Z_{ax\theta}} - \nu_a \frac{Z_{xx}}{Z_{axx}}\right) \end{bmatrix}$$

$$\begin{bmatrix} \kappa\cos(\kappa R_a)\left(\frac{Z_{\theta x}}{Z_{a\theta x}} - \nu_a \frac{Z_{\theta\theta}}{Z_{a\theta\theta}}\right) \\ \kappa\cos(\kappa R_a)\left(1 - \nu_a \frac{Z_{\theta x}}{Z_{a\theta x}} + \frac{Z_{\theta\theta}}{Z_{a\theta\theta}}\right) \end{bmatrix}^{-1} \begin{Bmatrix} d_{31} \\ d_{32} \end{Bmatrix} E_f \tag{6}$$

where, ν_a, d_{31} and d_{32} are the actuator Poisson ratio and PZT constants and E_f is the applied electric field. By using Eqs. 1 and 5, the actuator output forces and moments can be used to determine the structural response assuming the structural impedance is known. The computation of the structural response and structural impedance shall be presented next.

To determine the structural response of the SS cylinder caused by the actuation of the PZT actuator, a modal expansion analysis is performed. The equations that describe the motion of the cylinder are based on Love's equations for shell structures. The general equations have been adapted to incorporate loading caused by the actuation of line moments or forces[20]. Subsequently, the equations are developed to incorporate the loading generated by PZT actuators[17,18].

For a cylinder, the natural orthogonal modes can be used to determine the forced response using an infinite series:

$$u_i(x,\theta,t) = \sum_{k=1}^{\infty} p_k(t)U_{ik}(x,\theta)e^{i\omega t} \tag{7}$$

where, the subscript i corresponds to the associated displacement (i.e. $i=3$ represents transverse displacement), $p_k(t)$ represents the modal participation factor and $U_{ik}(x,\theta)$ is the spatial mode shape. For a SS cylinder the mode shape is given by[20]:

$$U_{1k}(x,\theta) = A_{mnp}\cos(\alpha x)\cos(n\theta) \tag{8a}$$

$$U_{2k}(x,\theta) = B_{mnp}\sin(\alpha x)\sin(n\theta) \tag{8b}$$

$$U_{3k}(x,\theta) = C_{mnp}\sin(\alpha x)\cos(n\theta) \tag{8c}$$

$$\alpha = \frac{m\pi}{l} \tag{8d}$$

where subscripts m and n represent the modal indices and subscript p refers to one of the three principal coordinates (1,2,3). After performing the standard modal expansion procedure to the differential equations (multiplying by the mode shape, integrating over the domain, and applying orthogonality conditions), the modal participation factor can be determined by solving an ordinary differential equation with a redefined forcing function:

$$\ddot{p}_k(t) + \omega_k^2 p_k(t) = F_k e^{i\omega t} \tag{9}$$

where, F_k is the a modified forcing function determined by the actuator forcing terms in the differential equation. The modified forcing function is defined in reference 20 and not included here for brevity. The solution to the modal participation factor can be given in the form:

$$p_k = \frac{F_k}{\omega_k^2 - \omega^2} \tag{10}$$

$$\vartheta = \frac{R}{\rho_s t_s N^*_{mnp}(\omega^2_{mnp} - \omega^2)}\left[-\frac{A_{mnp}}{C_{mnp}}\left(\frac{N_x}{n}\right) + \frac{B_{mnp}}{C_{mnp}}\left(\frac{N_\theta}{R\alpha} + \frac{M_\theta}{R^2\alpha}\right) + \left(\frac{N_\theta}{Rn\alpha} + \frac{M_x\alpha}{n} + \frac{M_\theta n}{R^2\alpha}\right)\right.$$

$$S_\theta = \sin n\theta_1 - \sin n\theta_2$$

$$C_\theta = \cos n\theta_1 - \cos n\theta_2$$

$$C_x = \cos \alpha x_1 - \cos \alpha x_2$$

where, N^*_{mnp} is the mode normalization constant:

inphase:

$$N^*_{mnp} = \frac{Rl\pi}{2}\left(\frac{A_{mnp}}{C_{mnp}}^2 + \frac{B_{mnp}}{C_{mnp}}^2 + 1\right) \quad n \neq 0, \quad m \neq 0$$

out of phase:

$$N^*_{mnp} = \frac{Rl\pi}{2}\left(\frac{B_{mnp}}{C_{mnp}}^2 + 1\right) \quad n \neq 0, \quad m \neq 0$$

The ratios A_{mnp}/C_{mnp} and B_{mnp}/C_{mnp} can be found in reference 20. Note that reference 18 and 19 have some typographical errors that have been corrected here. Finally the structural impedance needs to be described. For two dimensional structures, the admittance matrix is given by[19]:

$$\left(2\dot{u}\Big|_{inphase} - \varsigma\frac{\partial \dot{w}}{\partial x}\Big|_{outphase}\right)\Bigg|_{x=x_2} - \left(2\dot{u}\Big|_{inphase} - \varsigma\frac{\partial \dot{w}}{\partial x}\Big|_{outphase}\right)\Bigg|_{x=x_1} = -(H_{xx}F_x + H_{\theta x}F_\theta) \quad (12a)$$

$$\left(2\dot{v}\Big|_{inphase} - \varsigma\frac{\partial \dot{w}}{R\partial\theta}\Big|_{outphase}\right)\Bigg|_{\theta=\theta_2} - \left(2\dot{v}\Big|_{inphase} - \varsigma\frac{\partial \dot{w}}{R\partial\theta}\Big|_{outphase}\right)\Bigg|_{\theta=\theta_1} = -(H_{x\theta}F_x + H_{\theta\theta}F_\theta) \quad (12b)$$

where,

$$\varsigma = \frac{(t_s + t_a)^2}{2}$$

Based on the structural admittance defined in Eq. 12, the direct structural admittances are determined by dividing the axial or angular velocity by the appropriate force, F_x or F_θ. For brevity, only H_{xx} is presented. The remainder of the admittances can be found in reference 18 or 19.

$$H_{xx} = \frac{1}{R(\theta_2 - \theta_1)}\sum_{p=1}^{3}\sum_{m=1}^{\infty}\sum_{n=1}^{\infty}\left\{\left(\frac{\chi_{in}}{n}\left(\frac{A_{mnp}}{C_{mnp}}\right)^2 + \frac{\chi_{out}\alpha^2}{n}\right)(S_\theta \cos n\theta_o - C_\theta \sin n\theta_o)C_x\right\} \quad (13)$$

where,

$$\chi_{in} = -\frac{Ri\omega}{\rho_s t_s}\frac{2C_x}{N^*_{mnp}(\omega^2_{mnp} - \omega^2)}$$

$$\chi_{out} = -\frac{Ri\omega}{\rho_s t_s}\frac{(t_s + t_a)^2}{2N^*_{mnp}(\omega^2_{mnp} - \omega^2)}C_x$$

where θ_o refers to the actuator center. The structural admittance (Eq. 13) can now be used with Eq. 2 to determine the structural impedance, and therefore the actuator forces can be determined and substituted into Eq. 11 to determine the transverse displacement of the cylinder. It is the transverse velocity component of the cylinder that generates the acoustic field, and is what is of interest in this work. The calculation of the internal acoustic response shall be addressed next.

Acoustic Analysis

One way to compute the acoustic field produced by the vibration of a structure is to use the Kirchoff-Helmholtz (K-H) integral. If the structural surface vibration is the only source of acoustic energy, the K-H integral is given by[21]:

$$p(\vec{r}) = \int_S \left(p(\vec{r}_s)\frac{\partial G(\vec{r},\vec{r}_s)}{\partial n} + i\omega\rho_o \dot{w}_n(\vec{r}_s)G(\vec{r},\vec{r}_s)\right)dS \quad (14)$$

where, $p, \vec{r}, \vec{r}_s, n, \rho_o, \dot{w}_n, \& G$, represent the pressure, field point location, surface point location, outward normal to the local field velocity, density of the fluid medium (air), local normal surface velocity, and acoustic Green's function, respectively. The Green's function must satisfy the acoustic wave equation and the far-field radiation conditions. The K-H integral can then be directly integrated to solve for the acoustic field generated by a structure as long as the surface velocity and the surface pressure is known. Generally the spatial surface velocity of a structure can be measured or determined via finite element analysis or using analytical techniques. However, the spatial surface pressure is not easy to measure and is difficult to calculate.

Presently, acoustic boundary element analysis divides the surface into N elements and uses the integral to calculate the pressure at the surface. N simultaneous

equations need to be solved and this leads to some mathematical difficulties. Using the free-field Green's function, the integral contains singularities when $\vec{r} = \vec{r}_s$. For the radiation problem the formulation also fails to provide a unique solution to the surface pressure at interior acoustic eigen frequencies of the structural surface. Several methods have been presented to solve these difficulties for the radiation problem[22-26]. The solution of the internal problem however, has not received as much attention[7,27-30].

For the internal acoustic problem, a convenient form of the Green's function can facilitate in solving for the internal pressure field within a closed space. By choosing the Green's function such that,

$$\partial G/\partial n = 0 \tag{15}$$

The first integral in Eq. 14 is eliminated and the calculation of the surface pressure is no longer required. Therefore the pressure field can be solved by simply knowing the normal surface velocity of the structure. The Green's function that satisfies Eq. 15 is expressed in terms of the acoustical modes of the cavity and is given by[21]:

$$G(\vec{r},\vec{r}_s,\omega) = \sum_{ijk}^{\infty} \frac{\psi_{ijk}(\vec{r})\psi_{ijk}(\vec{r}_s)}{\Lambda_{ijk}(k_{ijk}^2 - k^2)c(\vec{r})} \tag{16a}$$

where,

$$c(\vec{r}) = \begin{cases} 1 & \text{within } V \\ 2 & \text{on the boundary of } V \end{cases} \tag{16b}$$

$$\Lambda_{ijk} = \int_V \psi_{ijk}^2(\vec{r})dV \tag{16c}$$

where ψ, k, Λ and subscript ijk are the internal acoustic mode shape, wavenumber, modal normalization constant and modal indices, respectively. For complicated geometries, the acoustic mode shape is difficult to compute and so direct calculation of Eq. 14 is generally not possible. However, for a finite closed cylinder the acoustic mode shapes and eigen values are known. The acoustic mode shape is given by[31]:

$$\psi_{ijk} = J_j(\lambda_{jk}\, r/R)\cos(i\pi x/l)\cos(j\theta) \tag{17}$$

where, J represents a j^{th} order Bessel function and λ are the associated roots of the Bessel function. The modal normalization constant is the mean square value of the acoustic mode shape multiplied by the volume of the cylinder. For a cylindrical duct the mean square value of 2-D mode shape is given for it's cross section[32]. This expression can be multiplied by the cylinder's axial mode shape and integrated over the length of the cylinder to yield:

$$\Lambda_{ijk} = \frac{J_j^2(\pi q_{jk})}{\varepsilon_i \varepsilon_j}\left\{1 - \frac{j^2}{(\pi q_{jk})^2}\right\} \tag{18}$$

where,

$$\varepsilon_i, \varepsilon_j = \begin{cases} 1 & i = 0, j = 0 \\ 2 & i > 0, j > 0 \end{cases}$$

and q_{jk} is related to the roots of the Bessel function. All the terms in the K-H integral (Eq. 14) have now been defined and the pressure within the cylinder can be determined directly. The only difficulty in this formulation is the singularity of the Green's function when the wavenumber coincides with one of the acoustic eigen frequencies of the cylinder. This can be addressed by including a small complex component in the acoustic wave speed[33].

Advantages/Disadvantages

The analysis presented in this work has several distinct advantages over existing techniques as well as some drawbacks. The structural response is based on a modal expansion formulation using the impedance model for PZT actuators. An impedance based model of the actuators is a significant improvement over existing models which do not consider the changing structural impedance of the cylinder with frequency. The analytical formulation also is much more flexible to changes in the parameters of the analysis (i.e. actuator size, position and loading) as compared to performing an equivalent finite element analysis (FEA). As with all structural analysis based on modal expansion (including FEA), the choice of damping affects the absolute response of the cylinder. Damping values are very difficult predict and have been shown to vary from one mode to the next. The analysis presented assumes a constant damping ratio and this constitutes an approximation. For the acoustic response, the direct integration of the K-H integral reduces the order of the problem as compared with using FEA. The analysis also circumvents calculating the surface pressure on the inside of the cylinder to determine internal acoustic response as is required by boundary element methods. This eliminates the singular integral caused when the field point coincides with the surface point. However, due to expanding the Green's function in terms of acoustic mode shapes, a singularity exists when the excitation frequency coincides with an eigen frequency of the enclosed cavity. The singularity is a mathematical deficiency and does not exist physically, but can be handled by introducing an imaginary component to the acoustic wave speed.

Experiment/Analysis

The experimental setup used to model a SS cylinder is shown in Fig. 4.

Figure 4. Experimental SS Cylinder with Collocated PZT Actuators Located at x=16/3", $\theta = 0^\circ$

The structure consists of an aluminum cylinder with two PZT actuators (G1195) collocated at x=16/3", $\theta = 0^\circ$, driven in phase. The boundary conditions are created by two thin aluminum annular shims (0.020" thick) and two thick aluminum circular disks (.5" thick, 8.75" diam.). The shims are screwed to the cylinder ends and bolted (w/epoxy) to the disks. Table 1 describes the properties of the instrumented cylinder. A roving accelerometer test was performed on the cylinder while the PZT's were driven (in phase) at 50 Vrms from 750 to 2250 Hz. A Kistler 86161A500 accelerometer was used to measure the cylinder response at x=l/4 and at x=l/2 for various angular positions (0, 15, 30,... 165, 180 deg.) which were mirrored about 180 deg. A Kistler 8620 accelerometer was used to measure the response at $\theta = 0^\circ$ for various axial positions (x=0, 1.33, 2.67, 4,... 14.67, 16 in.). The magnitude of the displacement response of the cylinder at zero angle for x=0, l/2, and l/4 can be seen in Fig. 5. The plot shows where the resonant frequencies of the cylinder occur and the mode which contributes the most to each resonance. The response at the ends (x = 0 & 16") is generally an order of magnitude less than the maximum transverse motion at a particular frequency. The other observation that can be made from Fig. 5 is that the accelerometer located at the cylinder's center does not detect motion at the (3,2), (4,2), and (2,2) modes.

Property*	Cylinder	PZT Actuator
Young's Modulus (Pa)	64×10^9	63×10^9
Density (Kg/m^3)	2700	7600
Poisson's Ratio	0.3	0.3
Loss Factor	0.005	0.001
Length (in.)	16	1.5
Outer Diameter (in)	10	-
Thickness (in.)	0.25	0.095
Width (in.)	-	1.24
Applied Voltage	-	50 Vrms
d_{32} (m/V)	-	-166×10^{-12}

* Note: All values should be converted to SI units

Table 1. Cylinder and Actuator Properties

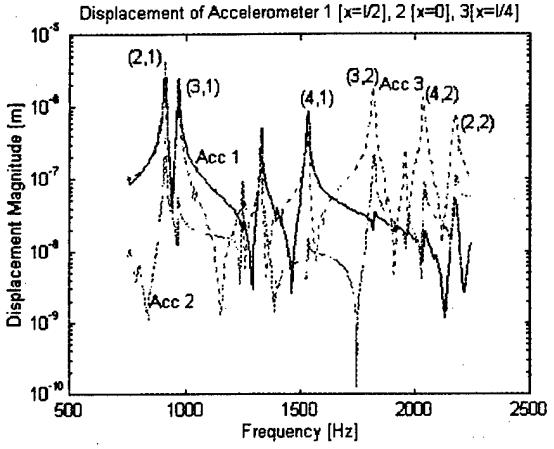

Figure 5. Cylinder Displacement at $\theta = 0$ deg.

The displacement magnitude at zero angle along the length of the cylinder is shown in Fig. 6. Clearly the low frequency resonances correspond to the axial "one" modes (i.e. (3,1) mode) and the higher frequency resonances correspond to the axial "two" modes (i.e. (4,2) mode). The other important observation that can be made from the plot is the small displacement occurring at the ends of the cylinder. This agrees with the theory that the boundary conditions are indeed simply-supported.

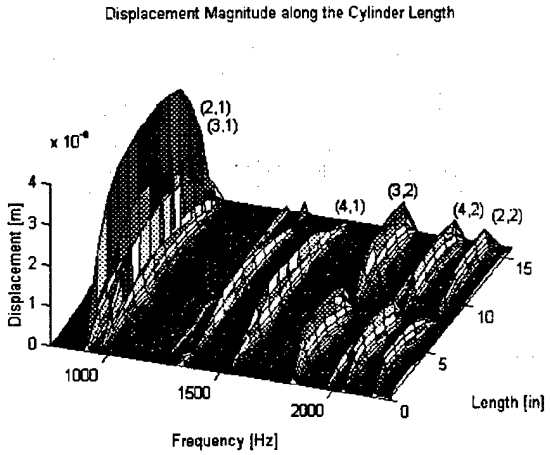

Figure 6. Spatial & Spectral Cylinder Displacement

The values of the modal indices have already been placed next to the associated resonance in Fig. 5 & 6 for clarity. However, the circumferential modal index for a

given frequency can not be determined without analyzing the circumferential displacement. For each of the resonant frequencies in Fig. 5, the circumferential displacement is determined. Figures 7-12 show the circumferential and axial displacement magnitude for a given resonant frequency. Based on the displacement patterns, the dominant modal index is determined. The experimental results indicate the cylinder is vibrating similar to a cylinder having simply-supported boundary conditions.

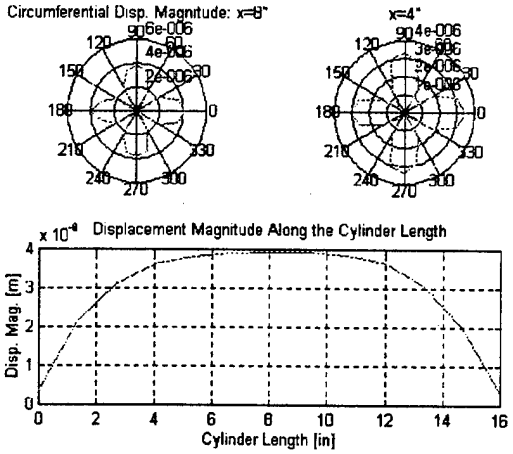

Figure 7. Cylinder Displacement at 910.5 Hz (2,1)

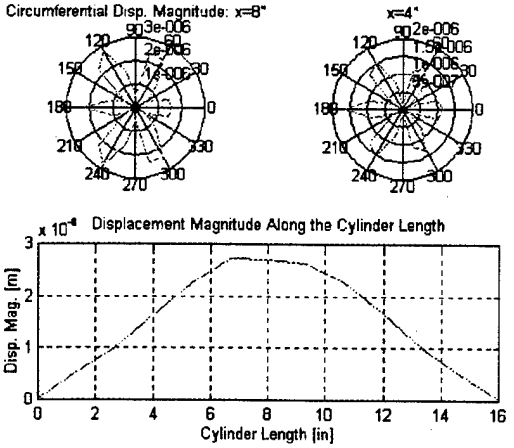

Figure 8. Cylinder Displacement at 965.7 Hz (3,1)

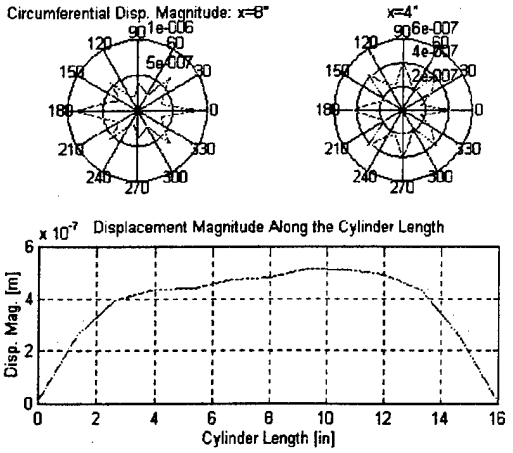

Figure 9. Cylinder Displacement at 1533 Hz (4,1)

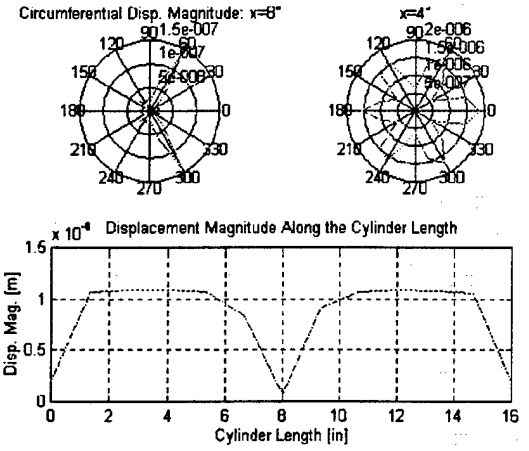

Figure 10. Cylinder Displacement at 1819 Hz (3,2)

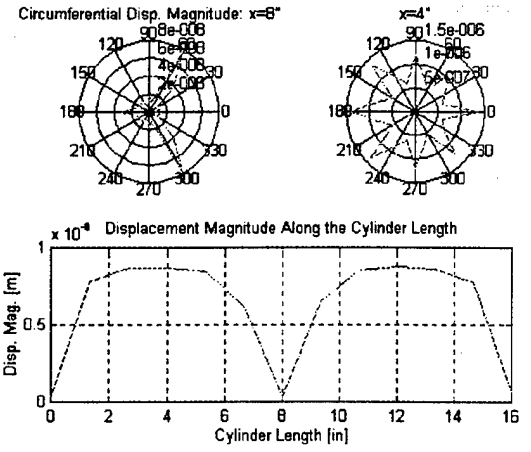

Figure 11. Cylinder Displacement at 2039 Hz (4,2)

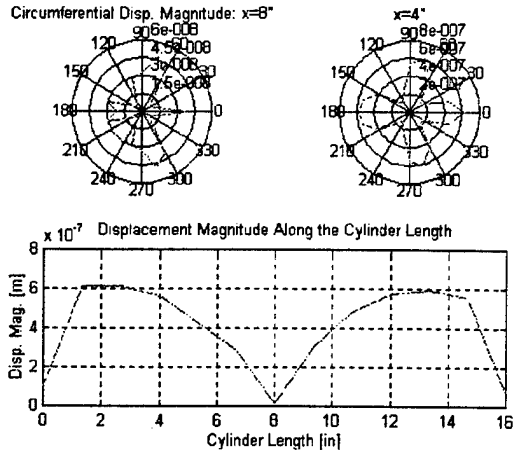

Figure 12. Cylinder Displacement at 2185 Hz (2,2)

The analytical structural model is used to predict the displacement response of the cylinder and is compared to the experimental results in Figures 13 and 14. Table 2 compares the natural frequencies of the analytical model based on Love's equations to the experimental results and also to the frequencies predicted by finite element analysis (FEA). The FEA was performed with the software I-DEAS using 30 axial and 72 circumferential thin shell elements. The analytical and FEA natural frequencies are in agreement to within less than 2.25% for all modes. The experimental resonant frequencies and the analytical natural frequencies are in excellent agreement for the (3,1), (4,1), and (4,2) modes. Less accurate coincidence is found for the (2,1), (3,2), and (2,2) modes. Some of these differences can be attributed to nine flats (1.5x1.25") that were milled on the outside of the cylinder to accomodate for other actuators. An extra resonant peak appears at 1328 Hz. This extra peak can be attributed to the non ideal boundary conditions. The only resonant frequency that has edge displacements of similar order as the axial maximum displacement occurs at 1328 Hz. It can therefore be concluded that this is a resonant frequency of the mechanical boundary (annular shim). The experimental and analytical responses of the cylinder do exhibit similar trends in the location of the resonant frequencies and in the influence of the actuator location on the response. Clearly the boundary conditions created in the experiment are not perfect; however they do provide a good comparison for the analytical model. More importantly for the acoustic problem, it is necessary for the structural analysis to be able to predict the amplitude of the velocity response. By inspecting Figures 13 and 14 it is clear that the analytical and experimental displacement magnitudes are very similar for the (3,1), (2,1), (4,1), (3,2), and (4,2) modes. This is of fundamental importance in order to determine the authority of PZT actuators for the rocket fairing problem.

Mode	Analytical	FEA	Exp.	% Error
(3,1)	981 (Hz)	973	966	1.5
(2,1)	1084	1082	911	19.0
(4,1)	1530	1525	1533	0.2
(3,2)	2022	2014	1819	11.1
(4,2)	2082	2060	2039	2.1
(1,1)	2190	2191	-	-
(5,1)	2378	2356	-	-
(5,2)	2740	2679	-	-
(2,2)	2798	2792	2185	27.6
(4,3)	3013	2946	-	-

Table 2. Comparison of Natural Frequencies

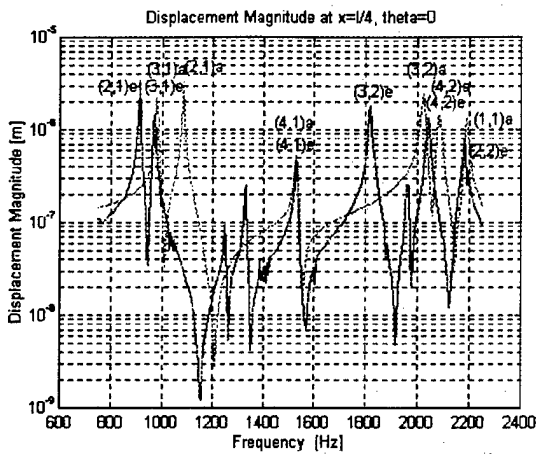

Figure 13. Analytical & Experimental Response at

$$x = l/4, \theta = 0^\circ$$

For the analytical natural frequencies which correspond to (4,1) and (3,2) modes, Fig. 15 and 16 show the analytical spatial displacement response. The

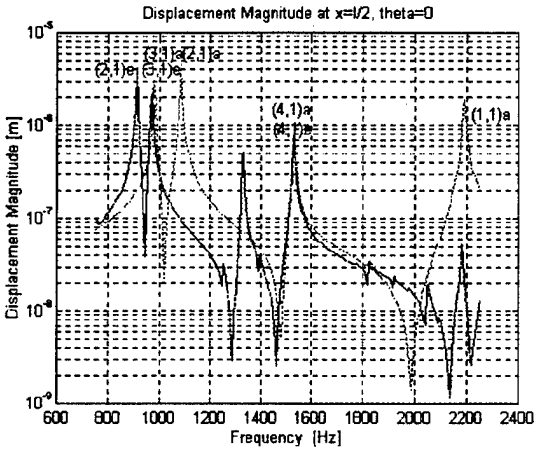

Figure 14. Analytical & Experimental Response at

$$x = l/2, \theta = 0^\circ$$

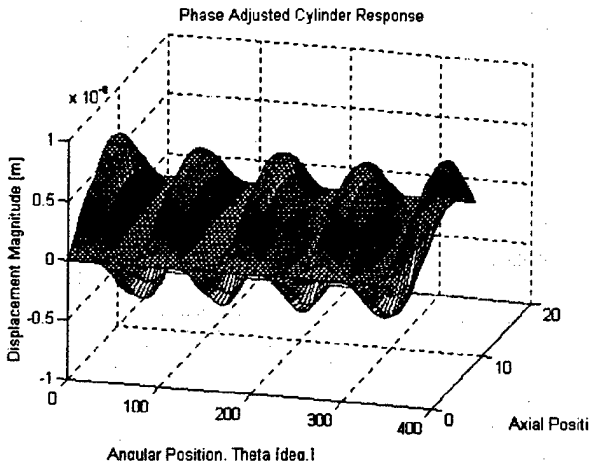

Figure 15. Analytical Response at 1533 Hz (4,1)

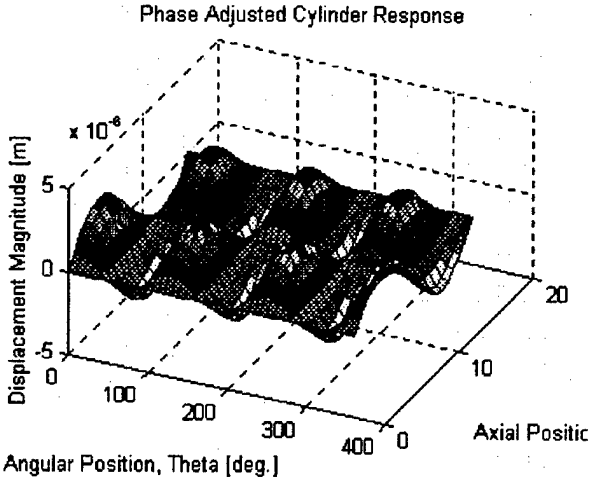

Figure 16. Analytical Response at 2021 Hz (3,2)

phase of the displacement response has been incorporated into the plots to show actual normal displacements. As is expected for each of these frequencies, the displacement response is similar to the dominant mode. The results indicate that the impedance model for PZT's actuating a SS cylinder can predict the overall resonant and modal behavior but, more importantly for acoustical applications, is able to determine the magnitude of the vibration.

Future Work

The structural model needs to be further verified for a broader frequency range with more experimental information about the absolute spatial displacement of the cylinder. This can be accomplished by using scanning laser vibrometry. The model also needs to be verified for out of phase actuation and more attention needs to be given to the actual damping values on a mode for mode basis. The results from the impedance model will ultimately be used to calculate the acoustic response within the cylinder. Once the acoustic model is verified, the combined structural/analytical model will be used to determine the authority of PZT actuators on a cylinder with properties similar to a rocket payload fairing.

Conclusions

An experiment of a cylinder with simply-supported boundary conditions has been conducted and was shown to exhibit dynamic behavior very similar to what the theory predicts. An analytical impedance based model of a PZT actuating on a SS cylinder was also described and compared with the experimental results. The results indicate that the impedance based model can predict the overall resonant and modal behavior but, more importantly for acoustical applications, is able to determine the magnitude of the vibration. An acoustical formulation of the pressure field within the cylinder has also been described based on the Kirchoff-Helmholtz integral. The work presented provides the initial steps required in determining the acoustic authority and feasibility of using piezoelectric actuators on rocket fairings.

Acknowledgments

This work is sponsored by the Air Force Office of Scientific Research grant #'s F49620-93-1-0280 and by F49620-94-1-0346 through the Center for Optimal Design and Control at VPI&SU. Thanks are given to Dr. Marc Jacobs (contract monitor), Dr. Alok Das & Capt. Jeanne Sullivan (Phillips Laboratory). Thanks are also extended to Dr. Frederic Lalande for his help in understanding the impedance model.

References

1. Long, M., Carne, D. A., Fuller, M. C., "Acoustic Blanket Effect on Payload Fairing Vibration," *Proceedings of the 42nd Annual Technical Meeting of the Institute of Environmental Sciences*, Orlando, Florida, May 12-17, 1996.

2. Bergen, T. F. & Kern, D. L., "Attenuation of the Cassini Spacecraft Vibroacoustic Environment," *Proceedings of the 42nd Annual Technical Meeting of the Institute of Environmental Sciences*, Orlando, Florida, May 12-17, 1996.

3. Hughes, W. O. & McNelis, A. M., "Cassini IV Acoustic Blanket Development and Testing," *Proceedings of the 42nd Annual Technical Meeting of*

the Institute of Environmental Sciences, Orlando, Florida, May 12-17, 1996.

4. Bradford, L. & Manning, J. E., "Acoustic Blanket Effect on Payload Acoustic Environment," *Proceedings of the 42nd Annual Technical Meeting of the Institute of Environmental Sciences*, Orlando, Florida, May 12-17, 1996.

5. Bergen, T. F., "Vibration Damping of the Cassini Spacecraft Structure," *Proceedings of the 41st Annual Technical Meeting of the Institute of Environmental Sciences*, Anaheim, CA, April 30-May 5, pp. 189-195, 1995.

6. Niezrecki, C. & Cudney, H. H., "Preliminary Review of Active Control Technology Applied to the Fairing Acoustic Problem," *Proceedings of the 39th Structures, Structural Dynamics and Materials Conference*, Salt Lake City, UT, 62-ASF-2, April 15-17, 1996.

7. Cheng, L., "Fluid-Structural Coupling of a Plate-Ended Cylindrical Shell: Vibration and Internal Sound Field," *Journal of Sound and Vibration*, **174**(5), pp. 641-654, 1994.

8. Lester, H. C. & Lefebvre, S., "Piezoelectric Actuator Models for Active Sound and Vibration Control of Cylinders," *Proceedings, Recent Advances in Active Noise and Vibration Control*, Blacksburg, VA, Technomic Publishing Company, Inc., 3-26, April 15-17, 1991.

9. Sonti, V. R. & Jones, J. D., "Active Vibration Control of Thin Cylindrical Shells Using Piezo-Electric Actuators," *Proceedings, Recent Advances in Active Noise and Vibration Control*, Blacksburg, VA, Technomic Publishing Company, Inc., 3-26, pp. 27-38, April 15-17, 1991.

10. Banks, H. T., Lester, H. C. & Smith, R. C., "A Piezoelectric Actuator Model for Active Vibration and Noise Control in Thin Cylindrical Shells," *Proceedings of the 31st Conference on Decision and Control*, Tuscon, Arizona, pp. 1797-1802, December, 1992.

11. Sonti, V. R. & Jones, J. D., "Curved Piezoelectric Model for Active Vibration Control of Cylindrical Shells," *AIAA Journal*, **34**(5), pp. 1034-1040, May, 1996.

12. Lalande, F., Chaudhry, Z. & Rogers, C. A., "Modeling Considerations for In-Phase Actuation of Actuators Bonded to Shell Structures," *Proceedings of the AIAA/ASME/ASCE/AHS/ASC 35th Structures, Structural Dynamics, and Materials Conference, Adaptive Structures Forum*, Hilton Head, SC, pp., 429-437, 1994.

13. Liang, C., Sun, F. P. & Rogers, C. A., "An Impedance Method for Dynamic Analysis of Active Material Systems," *Proceedings of the AIAA/ASME/ASCE/AHS/ASC 34th Structures, Structural Dynamics, and Materials Conference*, La Jolla, CA, pp. 3587-3599, 1993.

14. Zhou, S., Liang, C. & Rogers, C. A., "A Dynamic Model of a Piezoelectric Actuator-Driven Thin Plate," *Proceedings of the SPIE Conference on Smart Structures and Materials*, Orlando, FL, Vol. 2190, pp. 550-562, 1994.

15. Rossi, A., Liang, C. & Rogers, C. A., "Impedance Modeling of Piezoelectric Actuator-Driven Systems: An Application to Cylindrical Ring Structures," *Proceedings of the AIAA/ASME/ASCE/AHS/ASC 34th Structures, Structural Dynamics, and Materials Conference*, La Jolla, CA, pp. 3618-3624, 1993.

16. Lalande, F., Chaudhry, Z. & Rogers, C. A., "Comparison of Different Impedance-Based Models for Out-of-Phase Actuation of Actuators Bonded on Ring Structures," *Journal of Intelligent Material Systems and Structures*, Vol. 6, pp. 389-395, May, 1995.

17. Zhou, S., Liang, C. & Rogers, C. A., "Impedance Modeling of Two-Dimensional Piezoelectric Actuators Bonded on a Cylinder," *Proceedings of the ASME Winter Annual Meeting Adaptive Structures and Material Systems*, New Orleans, LA, AD-Vol. 35, pp. 247-255.

18. Lalande, F., Chaudhry, Z. & Rogers, C. A., "Impedance Based Modeling of Actuators Bonded to Shell Structures," *Journal of Intelligent Material Systems and Structures*, Vol. 6, pp. 389-395, November, 1995.

19. Lalande, F., "Modeling of Induced Strain Actuation of Shell Structures," Ph.D. Dissertation, Virginia Polytechnic Institute & State University, 1995.

20. Soedel, W., Vibrations of Shells and Plates, Marcel Dekker, Inc., New York, 1981.

21. Fahy, F., Sound and Structural Vibration, Academic Press, San Diego, CA, 1985.

22. Vasudevan, R. and Liu, Y. N., "Application of Integral Equations to Acoustic Problems," *Winter Annual Meeting of the ASME*, Atlanta, GA, NCA-Vol.

12/AMD-Vol. 128, Structural Acoustics, pp. 19-25, December 1-6, 1991.

23. Hahn, S. R., Ferri, A. A, Ginsberg, J. H., "A Review of Methods to Alleviate Non-Uniqueness in the Surface Helmholtz Integral Equation," *Winter Annual Meeting of the ASME*, Atlanta, GA, NCA-Vol. 12/AMD-Vol. 128, Structural Acoustics, pp. 223-234, December 1-6, 1991.

24. Latcha, M. A., Akay, A., "Application of the Helmholtz Integral in Acoustics," *Winter Annual Meeting of the ASME*, Anaheim, CA, ASME Paper 86-WA/NCA-31, pp. 1-7, 1986.

25. Burton, A. J. and Miller, G. F., "The Application of Integral Equation Methods to the Numerical Solution of Some Exterior Boundary-Value Problems," *Proceedings of the Royal Society of London*, A. 323, pp. 201-210, 1971.

26. Schenck, H. A., "Improved Integral Formulation for Acoustic Radiation Problems," *Journal of the Acoustical Society of America*, Vol. 44, pp. 41-58, 1968.

27. Francis, D. and Sadek, M. M., "An Integral Equation Method for Predicting Acoustic Emission Within Enclosures," *Proceedings of the Institution of Mechanical Engineers*, Vol. 199, No. C2, pp. 133-137, 1985.

28. Vlahopoulos, N., "A Numerical Structure-Borne Noise Prediction Scheme Based on the Boundary Element Method, with a New Formulation for the Singular Integrals," *Computers & Structures*, Vol. 50, No. 1, pp. 97-109, 1994.

29. Kipp, C. R. and Bernhard, R. J., "Prediction of Acoustical Behavior in Cavities Using an Indirect Boundary Element Method," *Journal of Vibration, Acoustics, Stress, and Reliability in Design*, Vol. 109, pp. 22-28, January, 1987.

30. Seybert, A. F. and Cheng, C., "Application of the Boundary Element Method to Acoustic Cavity Response and Muffler Analysis," *Winter Annual Meeting of the ASME*, Anaheim, CA, ASME Paper 86-WA/NCA-1, pp. 1-7, 1986.

31. Blevins, R. D., Formulas for Natural Frequency and Mode Shape, Robert E. Krieger Publishing Company, Malabar, FL, 1987.

32. Morse, P. M. and Ingard, K. U., Theoretical Acoustics, Princeton University Press, Princeton, NJ.

33. Silcox, R. J. and Lester, H. C., "Propeller Modeling Effects on Interior Noise In Cylindrical Cavities with Applications to Active Control," *AIAA 12th Aeroacoustics Conference*, San Antonio, TX, AIAA 89-1123, pp. 1-12, April 10-12, 1989.